Clean Technology for Resource, Energy and Environment

jcleantree.com

Research Article

Diffusion Dialysis Anion Exchange Membranes Based on a Polymer Blend with Compatibility Transition

Jinghao Guo[2], Xiaolong Tian[2], Mingkuo Sun[2], Tao Zhang[2], Wei Jiang[1,*], Danni Yang[2], Yulu Zhang[2,3], Tao Luo[2,*] and Xinlong Wang[2]

[1]*National Engineering and Technology Research Center for Development & Utilization of Phosphate Resources, Yunnan Phosphate Chemical Group Co., Ltd., Kunming 650699, China; Email: 357770174@qq.com*

[2]*Ministry of Education`s Research Center for Comprehensive Utilization and Clean Process Engineering of Phosphorous Resources, School of Chemical Engineering, Sichuan University, Chengdu 610065, China; Email: tao.luo@scu.edu.cn*

[3]*Membrane Separation and Resource Reutilization Laboratory, School of Chemical and Materials Engineering, Xuchang University, Xuchang 461000, Henan, China*

Cite This: https://doi.org/xxxxx-xxxxx-xxxxx

Read Online

ABSTRACT: Partially compatible polyphenylene oxide - polyvinyl pyrrolidone (PPO-PVP) dense membranes have been investigated for recovering sulfuric acid from salt-containing waste acid via diffusion dialysis. The compatibility of PPO-PVP blends with varying PVP (K90) contents was studied, and micro-phase separation behaviors were observed by transmission electron microscopy. In sulfuric acid solution, the carbonyl groups of pyrrolidone moieties react spontaneously with H^+, rendering the membrane positively charged and enabling anion exchange functionality. The mass transfer performance of membranes with different PVP mass ratios was studied. PPO-PVP blends are fully miscible at PVP contents ≤ 15 wt%, whereas distinct micro-phase separation occurs at 25–55 wt% PVP. The resultant membranes exhibit three micro-domains: PPO-rich domain, PVP-rich domain, and PVP aggregates, which are functionally distinguishable micro-domains rather than thermodynamic phases. The PVP aggregates act as ion transport channels within the membrane, and crucially, the membrane's mass transfer performance is highly dependent on the quantity and size of such PVP aggregates. The membrane with initial 45 wt% PVP delivers optimal performance (sulfuric acid permeability coefficient 34.9×10^{-9} $m^2\cdot h^{-1}$ and sulfuric acid/ferrous sulfate separation factor 17), arising from PPO-PVP compatibility transition-induced micro-phase separation that forms distinct micro-domains to mediate selective acid transport. This research reports an interesting compatibility transition phenomenon for the fabrication of micro-phase separated anion exchange membranes.

Keywords: Polymer blends; Anion exchange membranes; Diffusion dialysis; Micro-phase separation; Compatibility transition.

1. INTRODUCTION

Various modern industrial production processes generate a significant amount of acidic wastewater containing salt. For instance, in the titania (TiO2) production process using the sulfuric acid method, the production of 1 ton titania results in 6 ~ 8 tons of spent acid with 17 ~ 22 wt% H2SO4 and 40 ~ 60 tons of low-concentration acidic wastewater, along with the co-production of 3 ~ 3.5 tons of ferrous sulfate heptahydrate [1-3]. The predominant treatment methods for acidic wastewater containing salts [4] include high-temperature hydrolysis [5], neutralization precipitation [6], solvent extraction, evaporative crystallization [7], ion exchange [8], and membrane separation [8-10] (including electrodialysis [11,12] and diffusion dialysis [13-15]). For the treatment of salt-containing

Received: September 15, 2025
Accepted: October 25, 2025
Published: December 22, 2025

spent acid generated by the titania industry, the traditional limestone/lime neutralization precipitation method generates massive solid waste. Specifically, 7 ~ 12 tons of titanium gypsum are produced per ton of titania [16,17], which further gives rise to a series of problems including land occupation, water pollution, and resource waste[18]. Methods like ion exchange [19] and evaporative concentration [20] have not been widely adopted due to their high costs, energy consumption, and severe equipment corrosion [21]. Therefore, whether it is from an environmental protection perspective or a resource recycling perspective, the efficient treatment and valorization of salt-containing waste acid is the bottleneck that hampers the development of the titania industry.

Diffusion dialysis, based on ion exchange membranes, is an efficient separation technique characterized by its high selectivity, simple operation, and low energy consumption [22]. It has been widely studied in various applications, including the separation and recovery of sulfuric acid from copper-plated steel wire wastewater [23], purification of phosphoric acid from wet-process phosphoric acid [24,25], and separation of sulfuric acid and nickel sulfate from electroplating waste solutions [26]. Studies on the application of diffusion dialysis in the treatment of titania waste acid have been conducted [15,17]. However, due to the drawback of this process [27], this technology has not yet been widely implemented in industrial applications. One main challenge is the requirement of large membrane area, while this membrane is relatively expensive due to its complicated fabrication process. Thus, the pursuit of high-performance membranes with convenient fabrication process and wide material availability is important [28,29].

Polyphenylene oxide (PPO), a polymer of aryl chains, exhibits superior mechanical, chemical, and thermal stability versus typical aliphatic polymers [30,31]. With excellent film-forming capability and low cost, it is widely used in membrane research for energy [32,33], chemical engineering [34], and biomedical fields [35]. Conventionally, anion exchange membranes (AEMs) exhibit favorable acid diffusion coefficients and high acid/salt selectivity [36],[37]. He *et al*.[38] quaternize brominated PPO using 1,8-diazabicyclo[5.4.0]undec-7-ene to prepare AEMs for the separation of HCl-$FeCl_2$, achieving an acid permeance (U_{HCl}) of 27.0 × 10^{-3} m·h^{-1} and a separation factor (S) of 63. Lin *et al*. [13] fabricated porous AEMs for HCl-$FeCl_2$ separation, yielding U_{HCl} = 5.0 × 10^{-3} m·h^{-1} and S = 33. Their quaternized and brominated porous AEMs based on PPO [34] showed optimal permeance U_{HCl} = 7.0 × 10^{-3} m·h^{-1} and an acid/salt separation factor of 97. Khan *et al*. [39] quaternized brominated PPO with triphenylphosphine, achieving U_{HCl} ranging from 6.7 to 26.3 × 10^{-3} m·h^{-1} and the separation factor (S) ranging from 27 to 49 for HCl-$FeCl_2$ separation. However, these methods involve complex processes and hazardous reagents [40–42], leading to high membrane costs.

Polyvinyl pyrrolidone (PVP) is a commercially available, extensively studied polymer. Owing to strongly polar amide groups in its molecular structure, PVP is water-soluble (with polar group interactions), and features strong hydrogen-bonding/complex-forming capacities, as well as excellent solubility and film-forming properties. Zhang *et al*. [43] prepared completely miscible polyethersulfone-polyvinyl pyrrolidone (PES-PVP) blend dense AEMs that, under optimal conditions, achieved a sulfuric acid permeance $U_{H_2SO_4}$ = 3.0 × 10^{-3} m·h^{-1} and a sulfuric acid/ferrous sulfate separation factor S = 75. These mass transfer performance and selectivity are comparable to membranes prepared by conventional quaternization methods. Literature results [24,44] show that PES-PVP dense membranes undergo protonation and acquire fixed positive charges (as shown in Fig. **S1**) after being soaked in 2.0 M sulfuric acid at room temperature for 48 hours, endowing them with favorable selectivity. Based on the concept of polymer alloys, using hydrophilic-hydrophobic polymers miscible within a specific concentration range to prepare high-performance while low-cost polymer alloy AEMs via simple solution casting offers a potential approach to cutting membrane costs [43,45].

A previous study [45] characterized PPO-PVP (K10, K24, K40) miscibility via glass transition temperature, revealing distinct phase separation at 30 ~ 65 wt% PVP, with miscibility windows below 30 wt% or above 65 wt% PVP. The miscibility window's upper limit decreased with increasing PVP molecular weight. This miscibility transition induces unique physicochemical and optical properties in PPO-PVP heterogeneous blends, with phase-separated aggregates affecting membrane surface morphology and permeability [46].

Inspired by these studies, this research utilizes unmodified PPO as the hydrophobic component and PVP as the hydrophilic component to fabricate PPO-PVP blend membranes via solution casting. Acid soaking induces PVP protonation, spontaneously rendering the membranes as acid-recovery AEMs, enabling safe, cost-effective fabrication of diffusion dialysis AEMs. It also investigates how the PPO-PVP (K90) partial miscibility

affects membrane physicochemical properties and mass transfer performance, aiming to inform micro-phase separated membrane optimization and to clarify blend membranes structure-property relationship.

2. EXPERIMENTAL

2.1. Materials and Chemicals

PPO was kindly provided by Shandong Tianwei Membrane Technology Co., Ltd, with a number-average molecular weight of 25,600. PVP K90 was purchased from Macklin. Anhydrous ether was obtained from Jinshan Chemical Reagent Co., Ltd. Chloroform, ferrous sulfate heptahydrate, sulfuric acid, 0.1 M $KMnO_4$ standard solution, and 0.015 M Na_2CO_3 standard solution were purchased from Kelong Reagent Co., Ltd. The water employed in the experiments was deionized water from the laboratory's ultrapure water system. The purities and manufacturers of reagents are detailed in the Supporting Information, Table **S1**.

The simulated waste acid composition (2.68 M H_2SO_4 - 0.53 M $FeSO_4$) used for diffusion dialysis experiments was based on the composition of industrial titania waste acid from a company in Panzhihua City, Sichuan Province, China [43], whose composition is shown in Table **1**. For brevity, the simulated waste acid only contains sulfuric acid, ferrous sulfate and water.

The models and manufacturers of all experimental equipment and analytical instruments used are listed in the Supporting Information, Table (**S2**). Fig. (**1**) depicts photographs of the custom-made static diffusion dialysis experimental device (a) showing the internal structure of the device (b), as well as a schematic illustration of the operation mechanism during the static diffusion dialysis experiment (c).

2.2. Preparation and Pretreatment of Blend Membranes

2.2.1. Preparation of Casting Solution

Each portion of 42.5 g chloroform (solvent) was weighed and transferred into a bottle at room temperature. The PPO and PVP polymers used must be pre-dried using a vacuum drying oven (DZF-6020, NanJing HuiHeng Scientific Instrument Co., Ltd.) at 60°C for 12 hours. Following the composition specified in Table **2**, PPO and PVP were weighed and dissolved in chloroform, maintaining the total polymer mass fraction of the solution at 15 wt%. The mass ratio of PVP relative to the total polymer mass is varied to be 15, 25, 35, 45, 55, 65, and 75 wt%, respectively. The solution was stirred using a magnetic stirrer (DF-101S, Yuhua Instrument Co., Ltd.) at a speed of 300 rpm for 12 hours at room temperature to ensure the complete dissolution of PPO and PVP in chloroform.

Table 1: Composition of the industrial titania waste acid [43].

Component	H_2SO_4	$FeSO_4$	$Fe_2(SO4)_3$	$MgSO_4$	$TiOSO_4$	$Al_2(SO4)_3$	$MnSO_4$
Concentration (mol/L)	2.68	0.53	0.11	0.28	0.07	0.08	0.03

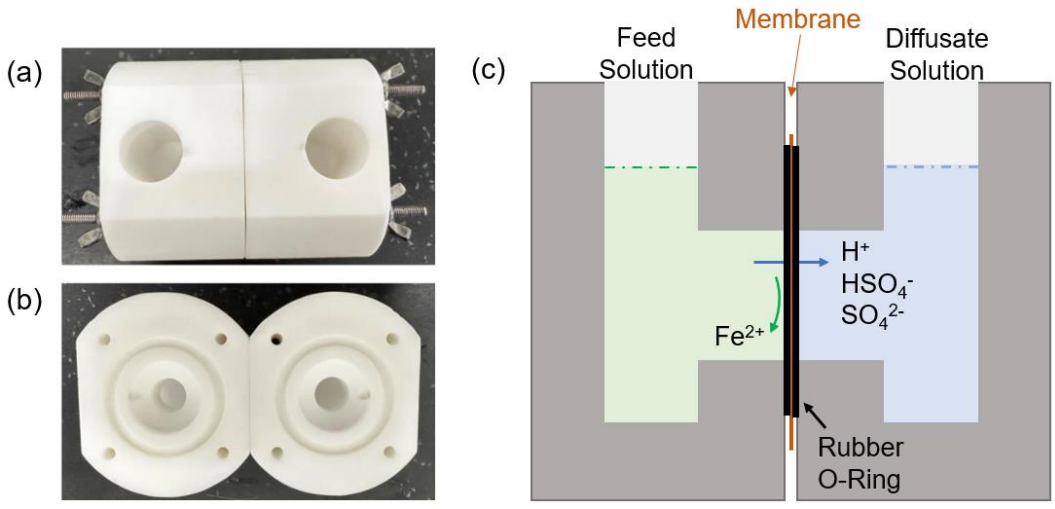

Figure 1: Photos of the custom-made static diffusion dialysis experimental device (**a**) displaying the internal structure (**b**), and schematic diagram of the operation mechanism (**c**).

Table 2: Composition of the polymer dope solutions for membrane casting.

PPO (g)	PVP (g)	PVP Content (wt%)	Chloroform (g)
6.375	1.125	15	42.5
5.625	1.875	25	42.5
4.875	2.625	35	42.5
4.125	3.375	45	42.5
3.375	4.125	55	42.5
2.625	4.875	65	42.5
1.875	5.625	75	42.5

2.2.2. Preparation and Acid Treatment of Blend Membranes

The polymer solution was subjected to a vacuum degassing procedure: it was placed within a vacuum drying oven and kept at ambient temperature to a pressure of - 60 kPa, followed by a 0.5-hour hold to remove dissolved gases. Subsequently, the gap of the doctor blade coater (KTQ-II, Tianjin Kexin Co., Ltd.) was adjusted to 500 μm. A certain volume of the casting solution was poured onto pre-cleaned and dried glass plates (30 × 30 × 1 cm), and the coating was applied using the coater. The wet polymer solution film on the glass plate was vacuum-dried at room temperature at -80 kPa for 24 hours to allow for the evaporation of chloroform. Once dried, the glass plates with the membranes were immersed in deionized water to facilitate the release of the dry membranes, which were then further dried in a convection oven (Model 101, Beijing YongGuangMing Medical Instrument Co., Ltd.) at 60°C for 12 hours to evaporate any residual moisture. The membranes thus obtained were denoted the as-prepared membranes. These membranes were then immersed in a simulated waste acid solution (2.68 M H_2SO_4 - 0.53 M $FeSO_4$) and, after a 48-hour immersion at room temperature, were ready for diffusion dialysis experiments. The preparation and post-treatment process of membranes is schematically shown in Fig. (**2**).

2.2.3. Annealing Treatment of Membranes

Membranes obtained via the evaporation of solvent under vacuum conditions may not have reached a thermodynamic equilibrium state in terms of the phase separation between PVP and PPO. Annealing treatment is expected to enhance the homogeneity of the membrane components or induce further phase separation until equilibrium. Preheat the vacuum drying oven, and place the membranes that have been dried to remove moisture into the vacuum drying oven. The membranes were subjected to a 4-hour constant temperature annealing process at 120°C. Afterwards, the membranes were allowed to cool naturally to room temperature inside the chamber. The annealed membranes were then subjected to acid soaking and diffusion dialysis experiments as described below.

2.3. Compatibility Analysis of PPO and PVP

2.3.1. Differential Scanning Calorimetry Analysis of PPO-PVP Blends

To investigate the compatibility of PPO and PVP K90, the freshly prepared casting solution was dropwise added to an excess of anhydrous ether. The precipitate was filtered and dried under vacuum at room temperature until a constant weight, resulting in PPO-PVP blend powders with different PVP contents.

The glass transition temperature (T_g) of the blend powders was determined using a thermogravimetric-differential scanning calorimetry instrument (DSC-200pc, NETZSCH, Germany). To eliminate the thermal history of the samples, a two-step heating method was employed, with the second heating curve chosen for further analysis.

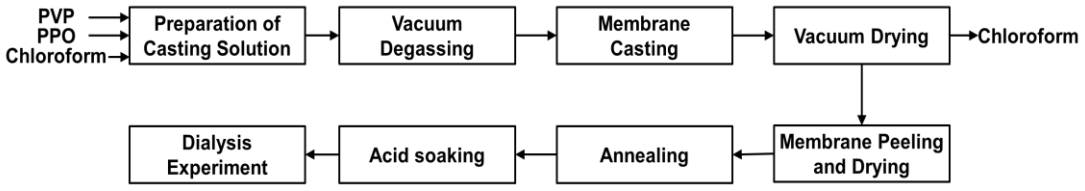

Figure 2: Schematic diagram of the PPO-PVP membrane preparation and characterization process.

Approximately 10 mg sample was loaded into a Al_2O_3 crucible and sealed, and the temperature was increased from 30 ℃ to 200 ℃ at a heating rate of 10 ℃/min under a nitrogen flow of 20 mL/min. After cooling to 50 ℃, the temperature was then increased from 50 ℃ to 400 ℃ at a heating rate of 10 ℃/min.

Additionally, the PPO-PVP blend membranes that had been fabricated were also subjected to DSC analyses. Membrane samples (2 × 2 mm in size) weighing about 10 mg were characterized using the same temperature program as described above, and the results based on the second heating curve were chosen.

2.3.2. Transmission Electron Microscopy (TEM) Characterization

To analyze the membrane microstructure and evaluate the compatibility of PVP with PPO, heat-annealed membrane samples with PVP contents of 35 and 45 wt% (had not been subjected to diffusion dialysis experiments) were selected. Ultra-thin slices of the samples, 50 ~ 70 nm in thickness, were prepared at room temperature using a Leica Microsystems-EM UC7 ultramicrotome. TEM images were then acquired using a transmission electron microscope (TEM, FEI-Tecnai G2 F30) operated at an acceleration voltage of 200 kV. The TEM images were analyzed to compare the microstructure and assess the miscibility of PPO and PVP.

2.4. Mass Transport Properties of the Membranes

Membranes subjected to acid soaking at room temperature for 48 hours were utilized for diffusion dialysis experiments to investigate the trans-membrane permeability of sulfuric acid and ferrous sulfate. The diffusion dialysis experiments were conducted in a custom-made device (Fig. **1**(**a**)), with an effective membrane area of 4.91 cm^2. The hydrated membrane thickness was measured using a digital micrometer (Mitutoyo, MDC-25PX), following which the membranes were installed into the experimental diffusion dialysis setup. 15 mL of simulated waste acid (2.68 M H_2SO_4 - 0.53 M $FeSO_4$) was added to one side of the dialysis cell, while 15 mL of deionized water was added to the other side. A magnetic stirrer was placed in each compartment and set to agitate at a speed of 400 rpm. After 3 hours, solution samples were taken from both the acid and water sides for analyzing the solution composition. The concentration of sulfuric acid was determined by titration with a 0.015 mol/L Na_2CO_3 solution, using methyl orange (1 g/L aqueous solution) as an indicator. Fe^{2+} was quantified by titration with a 0.1 mol/L $KMnO_4$ standard solution.

The permeance (U_i) and permeability coefficient (P_i) of H_2SO_4 and $FeSO_4$ were calculated using Equations 1 and 2, respectively, to compare the relative mass transport performance of the membranes. The separation factor (S) was determined using Equation 3, which was defined as the ratio of the permeance of H_2SO_4 to $FeSO_4$, indicating the membrane's selectivity towards H_2SO_4 over $FeSO_4$.

$$U_i = \frac{n_i}{At\Delta C_i} \tag{1}$$

$$P_i = U_i \cdot l \tag{2}$$

$$S_i = \frac{U_i(\mathrm{H_2SO_4})}{U_i(\mathrm{FeSO_4})} \tag{3}$$

In the equations, l is the thickness of the hydrated membrane (m), n_i denotes the amount of a particular component that has diffused to the water side (mol), A is the effective area of the membrane (m^2), t is the duration of the diffusion dialysis operation (h). ΔC_i is the average concentration of the solution in the two compartments (mol/m^3), and the calculation formula is as follows [15]:

$$\Delta C_i = \frac{c_f^0 - c_f^t - c_d^t}{\ln \frac{c_f^0 - c_d^t}{c_f^t}} \tag{4}$$

where c_f^0 and c_f^t are feed concentrations at time 0 and t, respectively, and c_d^t is the dialysate concentration at time t.

3. RESULTS AND DISCUSSION

3.1. The dope Solution and the Membrane Morphology

Fig. **3**(**a**) shows the optical photograph of the casting solutions immediately after preparation. As the PVP content increased, the casting solution became brighter however less transparent. After standing for around 12 hours, only the casting solutions with PVP contents of 15 wt% and 25 wt% were macroscopically observed to be homogeneous, while the others underwent liquid-liquid phase separation to varying extents (Fig. **3**(**b**)). The upper transparent phase is a PPO-rich solution that also contains a minor amount of PVP. The lower turbid phase is a more viscous solution rich in PVP. The solution with overall 75 wt% PVP content, predominantly exhibits the PVP-rich solution phase after standing. It can be preliminarily inferred that PVP and PPO are not

completely miscible at PVP K90 mass fractions of 35 ~ 75 wt%. In the freshly prepared solutions, the PVP and PPO polymers are mixed due to stirring, and phase separation occurs upon standing for some time (*eg.* 12 hours). To prevent such phase separation before the membrane-casting process, a 30-minute vacuum degassing operation was adopted instead of the 12-hour degassing process by standing.

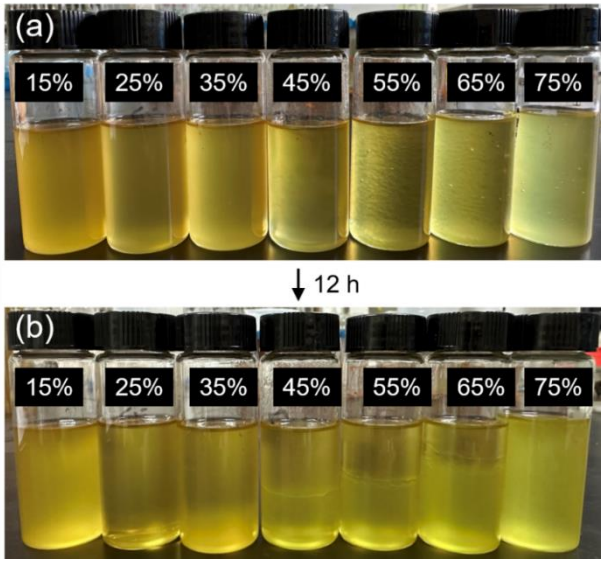

Figure 3: Optical photographs of the freshly prepared casting solutions (**a**) and those after standing 12 hours for degassing (**b**), the overall PVP mass ratios in the dope solutions are shown.

Fig. (**4**) presents optical photographs of the as-prepared blend membranes. The membranes containing PVP exhibit varying degrees of white turbidity (in contrast to the transparent pure PPO membranes, see Supporting Information, Fig. (**S2**)). This clearly indicates micro-phase separation within the PPO-PVP blend membranes, and suggests that (some) PVP is not uniformly distributed throughout the membrane matrix, while the results of scanning electron microscopic (SEM) characterization further confirm the existence of this micro-domain separation (see Supporting Information, Fig. (**S3**)) Under such circumstances, the membrane could achieve sulfuric acid permeation through two potential pathways: one is that a single domain formed by completely miscible PPO/PVP in the membrane, where the properties of PVP and PPO are combined, offering the stability of PPO along with the acid-absorbing capability of PVP, facilitating the trans-membrane transport of H_2SO_4; the other is that PVP forms a separate yet continuous domain in the membrane, creating an ion transport channel, enabling the trans-membrane permeation of sulfuric acid.

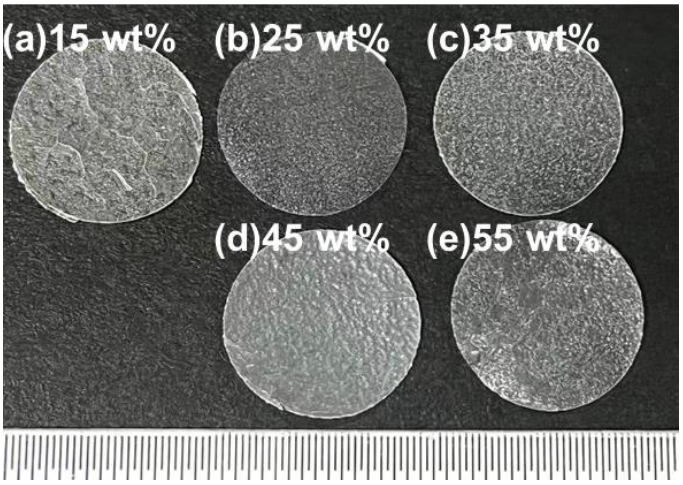

Figure 4: Optical photographs of the as-prepared dry PPO-PVP blend membranes, where (**a**) to (**e**) correspond to membranes with initial PVP contents of 15, 25, 35, 45, and 55 wt%, respectively. The scale resolution is 0.5 mm.

It should be noted that in this work, the initial PVP content refers to the mass fraction of PVP in the casting formulation, whereas the effective PVP content denotes the stabilized PVP fraction remaining in the membrane after the membrane has been exposed to water and acid solutions. When delaminating dried membranes from glass plates by immersion in water and subsequent soaking in simulated waste acid solutions, it was observed that blend membranes with overall PVP mass ratios of 45 ~ 65 wt% experienced partial PVP dissolution in water, those with 65 wt% dissolved in simulated waste acid solutions and in even water for the blend with 75 wt% PVP. Therefore, these blends with more than 65 wt% PVP are dimensionally unstable for use as membranes in diffusion dialysis. The membranes utilized for diffusion dialysis experiments include five types with PVP mass ratios of 15, 25, 35, 45, and 55 wt%. The membranes with initially 45 wt% and 55 wt% PVP after leaching out the unstable PVP were still employed for characterizing mass transport performance in diffusion dialysis experiments, although the actual PVP content had been reduced to below 45 wt% and 55 wt%.

3.2. Compatibility Analysis of PPO and PVP

3.2.1. Glass Transition Temperature of PPO-PVP Blends

The DSC curves of PPO, PVP K90, and PPO-PVP blend powders with different PVP contents were measured to determine the T_g and analyze the compatibility between PPO and PVP.

As shown in Fig. **5**(**a**), PVP K90, PPO, and PPO-PVP blend powder with 15 wt% PVP exhibited a single glass

transition temperature, indicating that PPO and PVP are compatible and can form a homogeneous domain when the PVP content is less than or equal to 15 wt%. In Fig. **5**(**b**), DSC curves of PPO-PVP blend powders with PVP contents of 25, 35, 45, 55, 65, and 75 wt% displayed two endothermic peaks, suggesting the presence of two glass transition temperatures in these PPO-PVP blend powders. The lower T_g in these curves is close to the T_g of PVP, while the higher T_g is close to the T_g of PPO. This phenomenon indicates the occurrence of micro-phase separation in the PPO-PVP blend powders with PVP contents of 25 ~ 75 wt%, indicating the inability to form a homogeneous domain. The DSC results of the PPO-PVP blend powders are consistent with the results shown in Fig. **3**(**b**). Based on the results from Fig. **3**(**b**) and Fig. **5**, it can be inferred that PVP K 90 and PPO might form a homogeneous domain when the PVP content is in the range of 15 ~ 25 wt%.

However, the DSC curves of the prepared PPO-PVP blend membranes are not as distinctly characterized as those of the blend powders (see Supporting Information, Fig. (**S4**) for the DSC curves of the PPO-PVP blend membranes). This may be attributed to the relaxation of molecular chain entanglements following annealing treatment, which reduces the heat capacity change during the glass transition of the samples.

3.2.2. Microscopic Structure of the Membranes

Analyzing the microscopic membrane structure via TEM and SEM (Fig. **S3**) allows us to examine the PVP distribution within the membrane. This analysis helps determine whether PVP forms continuous transport channels in the membrane to facilitate the transport of ions.

The TEM images depicted in Fig. **6**(**a,b,c,d**) reveal the presence of aggregates of varying sizes (50 ~ 200 nm, it should be noted that the size ranges are based on observations of representative TEM images rather than a statistical size distribution analysis) within the membrane containing overall 35 wt% PVP. The elemental distribution maps (f, g, h), in conjunction with the elemental analysis provided in the Supporting Information (Fig. **S5, S6**), confirm that these aggregates are enriched with PVP, resulting from PVP aggregation. Additionally, distinct domain boundaries are observable in the TEM images (c, d, e), indicating the presence of phase separation in the blend matrix. Judging from the elemental distribution, these interfaces are inferred to be the boundaries between PPO-rich and PVP-rich domain. It can be deduced that the PPO-rich domain, resembling PPO in nature, is hydrophobic, while the PVP-rich domain is hydrophilic. The PVP aggregates within the PVP-rich domain together serve as ion transport channels for the permeation of acid and salt.

The TEM images of the membrane with 45 wt% PVP are shown in Fig. (**7**), where (a), (b), (d), and (e) reveal two distinct domains within the PPO-PVP blend membrane. Clusters formed by the aggregation of PVP are observed. Compared to the blend membrane with 35 wt% PVP, the membrane with 45 wt% PVP exhibits a higher number density of PVP clusters, as evidenced by representative TEM observations. These clusters, together with the PVP-rich domain, are essential in the selective

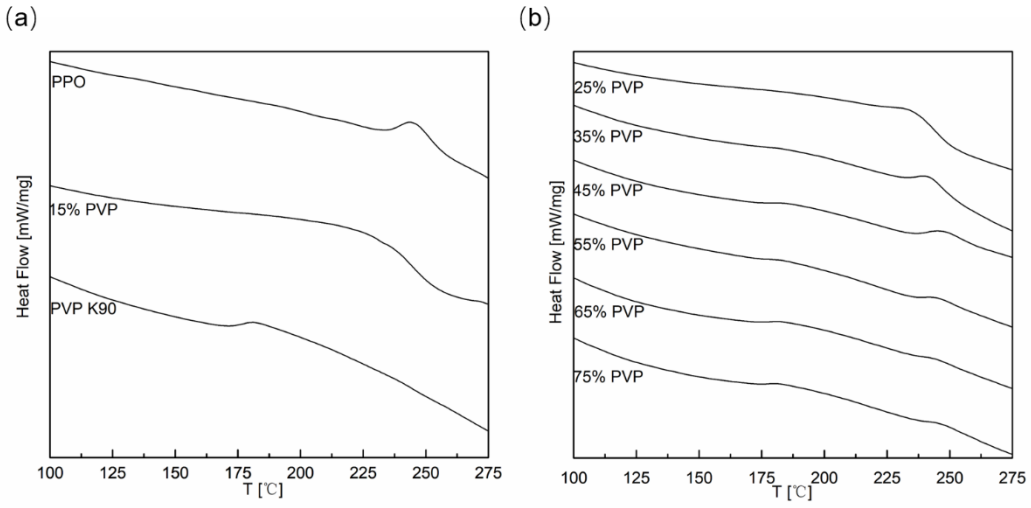

Figure 5: Differential scanning calorimetry (DSC) curves of PPO, PVP K90, and PPO-PVP blend powder with 15 wt% PVP K90 (**a**), DSC curves of PPO-PVP blend powders with PVP contents of 25, 35, 45, 55, 65, and 75 wt% (**b**).

permeation of sulfuric acid through the PPO-PVP blend membrane. The PVP clusters in both membranes (35 wt% and 45 wt% PVP) are predominantly located near the domain boundaries, likely due to the thermodynamic instability at the interface during phase separation between the PPO-rich domain and the PVP-rich domain. This instability, stemming from the uneven energy distribution at the interface, likely leads to the formation of heterogeneous nucleation sites and the aggregation of PVP.

Based on the above results, the final membrane morphology arises from the synergy of solution-phase miscibility, solvent evaporation, and post-annealing treatment. Partial miscibility between PPO and PVP in the casting solution determines the initial distribution of PPO-rich and PVP-rich regions. During solvent evaporation, this heterogeneity is kinetically frozen into the solid membrane, resulting in microphase-separated morphology. Subsequent annealing promotes further micro-phase separation toward a more thermodynamically stable morphology, leading to enlarged PVP aggregates and clearer micro-domain boundaries. These structural evolutions collectively govern ion transport behavior during diffusion dialysis.

3.3. Mass Transport Performance of Membranes

Fig. (**8**) presents the measured permeability coefficients of sulfuric acid and ferrous sulfate for the membranes before (a) and after (b) heat-annealing treatment. The membrane with 45 wt% PVP exhibits a significantly larger

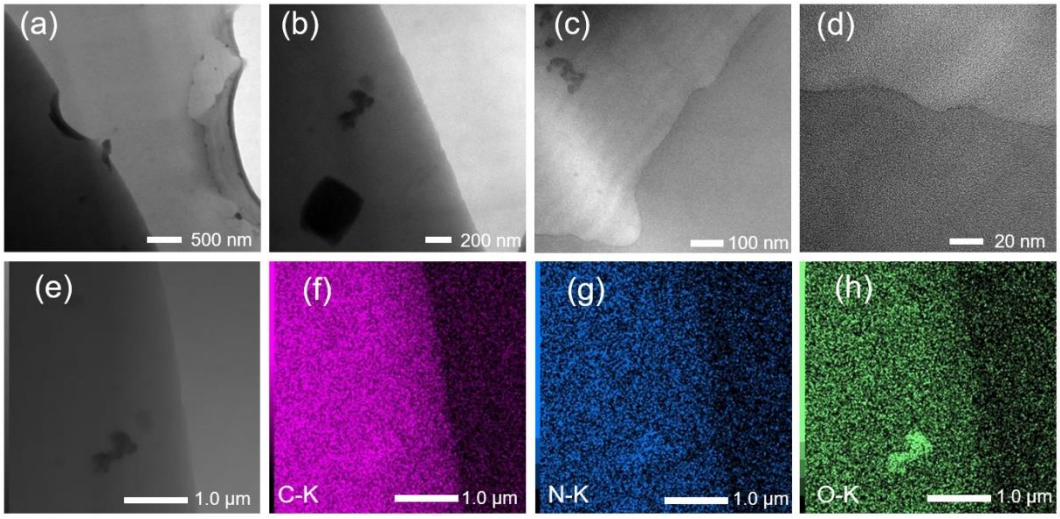

Figure 6: Transmission electron microscopic (TEM) images of the heat-annealed blend membrane with 35 wt% PVP (**a-e**); elemental distribution maps of the region shown in Fig. **6**(**e**): carbon element (**f**), nitrogen element (**g**), and oxygen element (**h**).

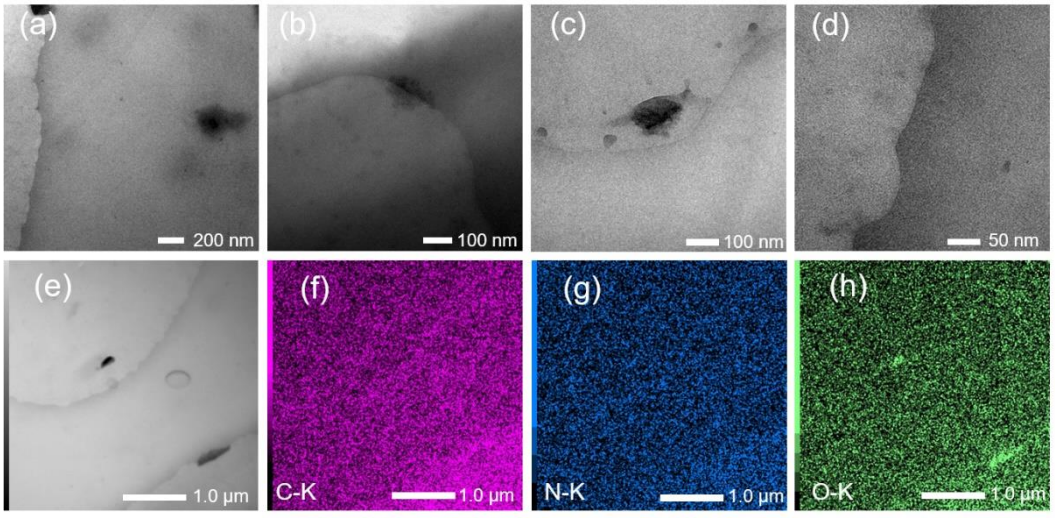

Figure 7: TEM images of the heat-annealed blend membrane with 45 wt% PVP (**a-e**); elemental distribution maps of the region in Fig. **7**(**e**): carbon element (**f**), nitrogen element (**g**), and oxygen element (**h**).

sulfuric acid permeability coefficient ($P_{H_2SO_4}$) compared to other membranes, while the ferrous sulfate permeability coefficient (P_{FeSO_4}) is only slightly larger than that of other membranes. Before annealing, $P_{H_2SO_4}$ is around 15.5×10^{-9} $m^2 \cdot h^{-1}$ and P_{FeSO_4} is about 1.5×10^{-9} $m^2 \cdot h^{-1}$, with a separation factor (S) of about 10. After annealing, $P_{H_2SO_4}$ increases to around $34.9 \times 10^{-9} m^2 \cdot h^{-1}$ and P_{FeSO_4} increases to about 2.1×10^{-9} $m^2 \cdot h^{-1}$, indicating a greater enhancement in the permeability coefficients of H_2SO_4 than $FeSO_4$. The separation factor also increases to 17, suggesting that the annealing process not only enhances the mass transport performance of the PPO-PVP membranes but also its selectivity. This enhancement could be attributed to the annealing treatment, which promoted phase separation within the membrane, leading to the enlargement of the PVP aggregate clusters and the formation of more ion transport channels. Additionally, the promotion of phase separation contributes to the formation of clearer domain boundaries, reducing non-selective ion transport due to ambiguous boundaries and thereby improving the membrane's $P_{H_2SO_4}$ and selectivity.

For membranes with PVP content ranging from 15 to 35 wt%, the values of $P_{H_2SO_4}$ and P_{FeSO_4} are very small. The membrane with the best mass transport performance within this range is the one with 35% PVP content. After annealing, $P_{H_2SO_4}$ is around 1.0×10^{-9} $m^2 \cdot h^{-1}$ and P_{FeSO_4} is about 0.24×10^{-9} $m^2 \cdot h^{-1}$, with a separation factor of 4.2. This indicates that within the 15 to 35 wt% PVP content range, the lower PVP content does not lead to the formation of many effective ion transport channels within the membrane, and the membrane's selectivity for H^+/Fe^{2+} is also not high.

At an initial PVP content of 55 wt%, a larger amount of PVP would theoretically be expected to form more ion transport channels; yet significant PVP leaching reduces the effective PVP content and compromises the hydrophilicity of the membrane. Consistent with this phenomenon, experimental results from diffusion dialysis show that the membranes with initial 55 wt% PVP do not exhibit larger permeability coefficients for either $P_{H_2SO_4}$ or P_{FeSO_4}, but rather lower than those of the membranes with initial 45 wt% PVP. Before annealing, $P_{H_2SO_4}$ is around 10.0×10^{-9} $m^2 \cdot h^{-1}$ and P_{FeSO_4} is about 1.9×10^{-9} $m^2 \cdot h^{-1}$, with a separation factor S of around 5. After annealing, $P_{H_2SO_4}$ decreases to around 3.6×10^{-9} $m^2 \cdot h^{-1}$ and P_{FeSO_4} decreases to about 0.26×10^{-9} $m^2 \cdot h^{-1}$. Both the permeability coefficients for H_2SO_4 and $FeSO_4$ decrease, while the separation factor increases to around 14. This suggests that in this case annealing also promotes phase separation, leading to clearer domain boundaries, but does not result in the formation of more effective ion transport channels by PVP aggregation. Instead, it reduces the efficiency of ion transport. This behavior can be attributed to the fact that excessive PVP leads to premature phase separation in the casting solution, followed by substantial PVP leaching during membrane stabilization, which ultimately disrupts continuous ion transport pathways. Elemental analyses revealed that the actual PVP content of the initial 45 wt% membrane (the effective membrane content is 14.37 wt%) after water washing was lower than that of the initial 55 wt% membrane (the effective membrane content is 24.28 wt%), and both were lower than the PVP content of initially 35 wt% membrane (the effective membrane content is provided in Table **S3**). The free volume remaining after PVP leaching can enhance H^+ permeability. For the membrane with an initial PVP content of 55 wt%, its PPO content is lower than that of the initial 45 wt% PVP membrane—this may reduce the supportive capacity of the membrane. Consequently, the free volume in the initial 55 wt% PVP membrane

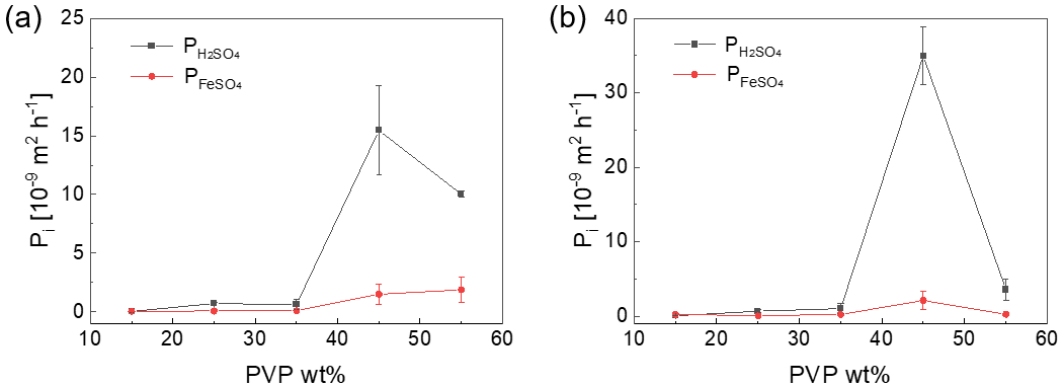

Figure 8: Permeability coefficients of sulfuric acid and ferrous sulfate for PPO-PVP blend membranes with different initial mass ratios of PVP, before (**a**) and after (**b**) heat-annealing treatment.

(following PVP leaching) are susceptible to collapse, which ultimately results in a lower $P_{H_2SO_4}$. The annealing treatment makes the membrane more compact, with PVP clusters being encapsulated by the hydrophobic PPO-rich domain, disrupting some ion transport channels and leading to a decline in the membrane's ion transport performance. Excessive PVP content compromises long-term stability via leaching. In contrast, 45 wt% initial PVP membranes exhibit good performance, attributed to a microphase separation–structural integrity balance driven by the PPO–PVP (K90) system's compatibility transition. Composition optimization and annealing alleviate PVP loss and enhance structural stability, highlighting that optimizing PVP content and microphase separation degree is pivotal for high-performance diffusion dialysis membranes. Post-fabrication treatment such as chemical crosslinking would enhance the stability of PVP in the blend membranes.

Thus, the optimal addition amount of PVP in the PPO-PVP blend membranes is about 45 wt%, at which the permeance of sulfuric acid $U_{H_2SO_4}$ is $0.4 \times 10^{-3} m \cdot h^{-1}$, and the permeability coefficient $P_{H_2SO_4}$ is about 34.9×10^{-9} $m^2 \cdot h^{-1}$. The acid/salt separation factor S is around 17. Compared to the AEMs mentioned in the Introduction, the ion transport performance of the PPO-PVP blend membranes is relatively lower. Notably interesting for this work, the PPO-PVP membranes, simply prepared through solution blending, possess a unique three-domain system, and its mass transport performance is unique due to the peculiar compatibility transition.

4. CONCLUSION

This work reports an interesting phenomenon observed for PPO and PVP blend membranes with peculiar permeability of sulfuric acid and ferrous sulfate. The PPO-PVP blend membranes with initially 45 wt% PVP have the largest permeability, even larger than those with initially 55 wt% PVP. These blend membranes are proposed as anion exchange membranes (AEMs) for the recovery of sulfuric acid from salt-containing waste acid via diffusion dialysis. The PPO and PVP blend membranes prepared with chloroform as the solvent and subsequent solvent evaporation form a microphase-separated structure, comprising a PPO-rich domain, a PVP-rich domain, and PVP aggregate clusters. The presence of PVP-rich domain enhances the hydrophilicity of the membrane, which facilitates the protonation of PVP and the acquisition of positive charges during acid soaking, rendering them as AEMs. The PVP aggregate clusters are important for achieving selective permeability in the PPO-PVP blend membranes. Results indicate that membranes with a larger number of PVP clusters exhibit significantly better mass transport performance than other membranes. Heat annealing treatment, which promotes micro-phase separation, further enhances the mass transport performance and selectivity of membranes with initially 45 wt% PVP. In contrast, the phase separation of the casting solution during the preparation of membranes with 55 wt% PVP content leads to suboptimal mass transport performance.

This study investigates the phase separation microstructure of PPO-PVP blend membranes and assesses their mass transport performance. It reveals correlation between the microstructure and mass transport performance of micro-heterogeneous PPO-PVP blend membranes, offering reference to fabricating AEMs for diffusion dialysis using partially miscible commodity polymers.

CONFLICT OF INTERESTS

The authors declare no conflict of interests.

ACKNOWLEDGEMENTS

The authors acknowledge the financial support from the "National Engineering and Technology Research Center for Development & Utilization of Phosphate Resources" in China (Grant NO. NECP2023-05).

REFERENCES

[1] Liu Z, Dong J, Feng Y, Li H. Reuse of waste acid from titanium dioxide industry: Efficient synthesis and functional exploration of titanium phosphate. Chem Phys Lett 2023;833:140938. https://doi.org/10.1016/j.cplett.2023.140938.

[2] Matei E, Predescu AM, Șăulean AA, Râpă M, Sohaciu MG, Coman G, *et al*. Ferrous Industrial Wastes—Valuable Resources for Water and Wastewater Decontamination. Int J Environ Res Public Health 2022;19:13951. https://doi.org/10.3390/ijerph192113951.

[3] Zhang Y, Yang D, Peng B, Luo T, Yang X, Yang L, *et al*. Miscibility and Hydrophobicity of Pyrrolidone-Containing Copolymers Determine Blend Membrane Properties for Diffusion Dialysis. ACS Appl Polym Mater 2025;7:3872–82. https://doi.org/10.1021/acsapm.5c00108.

[4] Regel-Rosocka M. A review on methods of regeneration of spent pickling solutions from steel processing. J Hazard Mater 2010;177:57–69. https://doi.org/10.1016/j.jhazmat.2009.12.043.

[5] Zhou S, Qian B, Hosseini T, De Girolamo A, Zhang L. Pyrohydrolysis of $CaCl_2$ Waste for the Recovery of HCl Acid upon the Synergistic Effects from $MgCl_2$ and Silica. ACS Sustain Chem Eng 2019;7:3349–55. https://doi.org/10.1021/acssuschemeng.8b05513.

[6] Li L, Li S, Dong Y, Yang P, Wang R. Pilot Study on the Deep Treatment of Sulfuric-Acid–Titanium-Dioxide Wastewater Using an Ultrafiltration/Reverse Osmosis Process. Processes 2023;11:1626. https://doi.org/10.3390/pr11061626.

[7] Tian Q, Li G, Xin Y, Lv X, Lv X, Yu W, *et al*. Comprehensive treatment of acid effluent containing antimony and arsenic by selective reduction and evaporative crystallization.

Hydrometallurgy 2020;195:105366. https://doi.org/10.1016/j.hydromet.2020.105366.

[8] Nenov V, Dimitrova N, Dobrevsky I. Recovery of sulphuric acid from waste aqueous solutions containing arsenic by ion exchange. Hydrometallurgy 1997;44:43–52. https://doi.org/10.1016/S0304-386X(96)00029-1.

[9] Mautner A. Nanocellulose water treatment membranes and filters: a review. Polym Int 2020;69:741–51. https://doi.org/10.1002/pi.5993.

[10] Obotey Ezugbe E, Rathilal S. Membrane Technologies in Wastewater Treatment: A Review. Membranes 2020;10:89. https://doi.org/10.3390/membranes10050089.

[11] Caprarescu S, Corobea MC, Purcar V, Spataru CI, Ianchis R, Vasilievici G, *et al*. San copolymer membranes with ion exchangers for Cu(II) removal from synthetic wastewater by electrodialysis. J Environ Sci 2015;35:27–37. https://doi.org/10.1016/j.jes.2015.02.005.

[12] Căprărescu S, Modrogan C, Purcar V, Dăncilă AM, Orbuleț OD. Study of Polyvinyl Alcohol-SiO2 Nanoparticles Polymeric Membrane in Wastewater Treatment Containing Zinc Ions. Polymers 2021;13:1875. https://doi.org/10.3390/polym13111875.

[13] Yang J, Dai G, Wang J, Pan S, Lu G, Shi X, *et al*. Porous Anion Exchange Membrane for Effective Acid Recovery by Diffusion Dialysis. Processes 2021;9:1049. https://doi.org/10.3390/pr9061049.

[14] Gong Y, Shen H, Zhao H, Zhang Y, Li P, Cheng C. Excellent dimensional stability anion exchange membrane based on PVA/EVOH/PyPECH for acid recovery by diffusion dialysis. J Environ Chem Eng 2024;12:112315. https://doi.org/10.1016/j.jece.2024.112315.

[15] Tongwen X, Weihua Y. Sulfuric acid recovery from titanium white (pigment) waste liquor using diffusion dialysis with a new series of anion exchange membranes — static runs. J Membr Sci 2001;183:193–200. https://doi.org/10.1016/S0376-7388(00)00590-1.

[16] Dai Y, Dong H, Sun L, Li J, Zhang T, Geng Y, *et al*. Life cycle environmental impact assessment of titanium dioxide production in China. Environ Impact Assess Rev 2024;105:107412. https://doi.org/10.1016/j.eiar.2023.107412.

[17] Yang D, Luo T, Zhang T, Lv L, Zou Z, Tang S. Miscible Polymer Blend Membranes Bearing Pyrrolidone for Fractioning Sulfuric Acid and Sulfates. Polym Adv Technol 2025;36:e70079. https://doi.org/10.1002/pat.70079.

[18] Ma Y, Hu C, Jin Y, Zhen H, Wu J, Yang L. Recovery of ruthenium resources from red mud via phosphoric acid leaching: A comprehensive investigation of leaching effects and kinetics. J Clean Prod 2025;486:144423. https://doi.org/10.1016/j.jclepro.2024.144423.

[19] Feng X, Jiang LY, Song Y. Titanium white sulfuric acid concentration by direct contact membrane distillation. Chem Eng J 2016;285:101–11. https://doi.org/10.1016/j.cej.2015.09.064.

[20] Qiu H, Wang M, Xie Y, Song J, Huang T, Li X-M, *et al*. From trace to pure: Recovery of scandium from the waste acid of titanium pigment production by solvent extraction. Process Saf Environ Prot 2019;121:118–24. https://doi.org/10.1016/j.psep.2018.10.027.

[21] Han F, Wang M, Liu W, Song W. Recovery of sulfuric acid and iron from titanium dioxide waste acid by membrane electrolysis combined with selective electrodialysis. Sep Purif Technol 2024;344:127199. https://doi.org/10.1016/j.seppur.2024.127199.

[22] Luo J, Wu C, Xu T, Wu Y. Diffusion dialysis-concept, principle and applications. J Membr Sci 2011;366:1–16. https://doi.org/10.1016/j.memsci.2010.10.028.

[23] Loza S, Loza N, Korzhov A, Romanyuk N, Kovalchuk N, Melnikov S. Hybrid Membrane Technology for Acid Recovery from Wastewater in Coated Steel Wire Production: A Pilot Scale Study. Membranes 2022;12:1196. https://doi.org/10.3390/membranes12121196.

[24] Zhang Q, Dong Q-F, Zheng M-S, Tian Z-W. The preparation of a novel anion-exchange membrane and its application in all-vanadium redox batteries. J Membr Sci 2012;421–422:232–7. https://doi.org/10.1016/j.memsci.2012.07.024.

[25] He F, Zhou X, Luo T, Wang X. Study on the preparation of high-concentration ammonium phosphate suspension fertilizer from wet-process phosphoric acid and its rheological properties. J Taiwan Inst Chem Eng 2024;161:105497. https://doi.org/10.1016/j.jtice.2024.105497.

[26] Loza S, Loza N, Kovalchuk N, Romanyuk N, Loza J. Comparative Study of Different Ion-Exchange Membrane Types in Diffusion Dialysis for the Separation of Sulfuric Acid and Nickel Sulfate. Membranes 2023;13:396. https://doi.org/10.3390/membranes13040396.

[27] Yan J, Wang H, Fu R, Fu R, Li R, Chen B, *et al*. Ion exchange membranes for acid recovery: Diffusion Dialysis (DD) or Selective Electrodialysis (SED)? Desalination 2022;531:115690. https://doi.org/10.1016/j.desal.2022.115690.

[28] Singh G, Yadav G, Yadav N, Kapoor S, Sharma B, Sharma RK, *et al*. Recent advancements in the synthesis of anion exchange membranes and their potential applications in wastewater treatment. Adv Colloid Interface Sci 2025;336:103376. https://doi.org/10.1016/j.cis.2024.103376.

[29] Wu L, Luo T, Yang X, Zhao H, Wang X, Zhang Z. Impact of the Donnan electrolytes on selectivity of cation exchange membranes evaluated via the ionic membrane conductivity. Sep Purif Technol 2023;316:123816. https://doi.org/10.1016/j.seppur.2023.123816.

[30] Dmitrenko M, Chepeleva A, Liamin V, Mazur A, Semenov K, Solovyev N, *et al*. Novel Mixed Matrix Membranes Based on Polyphenylene Oxide Modified with Graphene Oxide for Enhanced Pervaporation Dehydration of Ethylene Glycol. Polymers 2022;14:691. https://doi.org/10.3390/polym14040691.

[31] Larrañaga M, Serrano E, Martin MD, Tercjak A, Kortaberria G, De La Caba K, *et al*. Mechanical properties–morphology relationships in nano-/microstructured epoxy matrices modified with PEO–PPO–PEO block copolymers. Polym Int 2007;56:1392–403. https://doi.org/10.1002/pi.2289.

[32] Basso Peressut A, Montagna J, Moretti P, Arrigoni A, Latorrata S, Bertarelli C, et al. Development and characterization of crosslinked PPO-based anion exchange membranes for AEM fuel cells. Solid State Ion 2023;394:116212. https://doi.org/10.1016/j.ssi.2023.116212.

[33] Hickner MA, Ghassemi H, Kim YS, Einsla BR, McGrath JE. Alternative Polymer Systems for Proton Exchange Membranes (PEMs). Chem Rev 2004;104:4587–612. https://doi.org/10.1021/cr020711a.

[34] Lin J, Huang J, Wang J, Yu J, You X, Lin X, *et al*. High-performance porous anion exchange membranes for efficient acid recovery from acidic wastewater by diffusion dialysis. J Membr Sci 2021;624:119116. https://doi.org/10.1016/j.memsci.2021.119116.

[35] Zhou J, Zuo P, Liu Y, Yang Z, Xu T. Ion exchange membranes from poly(2,6-dimethyl-1,4-phenylene oxide) and related applications. Sci China Chem 2018;61:1062–87. https://doi.org/10.1007/s11426-018-9296-6.

[36] Khodabakhshi AR, Madaeni SS, Hosseini SM. Preparation and characterization of monovalent ion-selective poly(vinyl chloride)- *blend* -poly(styrene- *co* -butadiene) heterogeneous anion-exchange membranes. Polym Int 2011;60:466–74. https://doi.org/10.1002/pi.2970.

[37] Tuli SK, Roy AL, Elgammal RA, Zawodzinski TA, Fujiwara T. Polystyrene-based anion exchange membranes via click chemistry: improved properties and AEM performance. Polym Int 2018;67:1302–12. https://doi.org/10.1002/pi.5657.

[38] He Y, Pan J, Wu L, Ge L, Xu T. Facile preparation of 1,8-Diazabicyclo[5.4.0]undec-7-ene based high performance anion exchange membranes for diffusion dialysis applications. J

Membr Sci 2015;491:45–52. https://doi.org/10.1016/j.memsci.2015.04.055.

[39] Khan MI, Khraisheh M, AlMomani F. Innovative BPPO Anion Exchange Membranes Formulation Using Diffusion Dialysis-Enhanced Acid Regeneration System. Membranes 2021;11:311. https://doi.org/10.3390/membranes11050311.

[40] Emmanuel K, Cheng C, Erigene B, Mondal AN, Hossain MdM, Khan MI, *et al*. Imidazolium functionalized anion exchange membrane blended with PVA for acid recovery via diffusion dialysis process. J Membr Sci 2016;497:209–15. https://doi.org/10.1016/j.memsci.2015.09.043.

[41] Wang P, Wu C, Sun M, Zhang X, Wu Y. Porous P84 co-polyimide anion exchange membranes for diffusion dialysis application to recover acids. Desalination Water Treat 2018;108:40–8. https://doi.org/10.5004/dwt.2018.21949.

[42] Liu W, Li M, Sun M, Zhang X, Wu C, Wu Y. Graphene oxide modified porous anion exchange membranes for acid recovery through diffusion dialysis. Desalination Water Treat 2020;175:49–59. https://doi.org/10.5004/dwt.2020.24903.

[43] Zhang Y, Song G, Luo T, Yang X, Ren H, Wang X, *et al*. Acid-triggered polyether sulfone - Polyvinyl pyrrolidone blend anion exchange membranes for the recovery of titania waste acid via diffusion dialysis. J Membr Sci 2022;662:120980. https://doi.org/10.1016/j.memsci.2022.120980.

[44] Zhang Y, Luo T, Yang X, Wang X, Zhang Z. Superior diffusion dialysis anion exchange membranes from miscible polyether sulfone – poly(vinyl pyrrolidone-co-styrene) blends. J Membr Sci 2023;680:121704. https://doi.org/10.1016/j.memsci.2023.121704.

[45] Goh SH, Lee Shern Lim. Miscibility of poly(2,6-dimethyl-1,4-phenylene oxide) with poly(p-methylstyrene-co-acrylonitrile). Eur Polym J 1990;26:711–4. https://doi.org/10.1016/0014-3057(90)90234-U.

[46] Kaur S, Kumar P, Thangaraj R. Phase immiscibility induced enhanced fluorescence in spin-coated PVP/PPO polyblends. Polym Bull 2013;70:2269–76. https://doi.org/10.1007/s00289-013-0948-6.